Dual-purpose BGaN layers on performance of nitride-based high electron mobility transistors

Vinod Ravindran, Mohamed Boucherit, Ali Soltani, Simon Gautier, Tarik Moudakir, Jeramy Dickerson, Paul L. Voss, Marie-Antoinette Di Forte-Poisson, Jean-Claude de Jaeger, Abdallah Ougazzaden

▶ **To cite this version:**

Vinod Ravindran, Mohamed Boucherit, Ali Soltani, Simon Gautier, Tarik Moudakir, et al.. Dual-purpose BGaN layers on performance of nitride-based high electron mobility transistors. Applied Physics Letters, 2012, 100, pp.243503-1-4. 10.1063/1.4729154 . hal-00787871

HAL Id: hal-00787871
https://hal.science/hal-00787871

Submitted on 27 May 2022

HAL is a multi-disciplinary open access archive for the deposit and dissemination of scientific research documents, whether they are published or not. The documents may come from teaching and research institutions in France or abroad, or from public or private research centers.

L'archive ouverte pluridisciplinaire **HAL**, est destinée au dépôt et à la diffusion de documents scientifiques de niveau recherche, publiés ou non, émanant des établissements d'enseignement et de recherche français ou étrangers, des laboratoires publics ou privés.

Applied Physics Letters

Dual-purpose BGaN layers on performance of nitride-based high electron mobility transistors

Cite as: Appl. Phys. Lett. **100**, 243503 (2012); https://doi.org/10.1063/1.4729154
Submitted: 27 March 2012 • Accepted: 20 May 2012 • Published Online: 13 June 2012

Vinod Ravindran, Mohamed Boucherit, Ali Soltani, et al.


View Online


Export Citation

ARTICLES YOU MAY BE INTERESTED IN

Bandgap bowing in BGaN thin films
Applied Physics Letters **93**, 083118 (2008); https://doi.org/10.1063/1.2977588

Wurtzite BAlN and BGaN alloys for heterointerface polarization engineering
Applied Physics Letters **111**, 222106 (2017); https://doi.org/10.1063/1.5008451

Neutron detection using boron gallium nitride semiconductor material
APL Materials **2**, 032106 (2014); https://doi.org/10.1063/1.4868176

Lock-in Amplifiers up to 600 MHz
Zurich Instruments
Watch

AIP Publishing

© 2012 American Institute of Physics.

Dual-purpose BGaN layers on performance of nitride-based high electron mobility transistors

Vinod Ravindran,[1,2] Mohamed Boucherit,[3] Ali Soltani,[3] Simon Gautier,[2,4] Tarik Moudakir,[2] Jeramy Dickerson,[1,2] Paul L. Voss,[1,2] Marie-Antoinette di Forte-Poisson,[5] Jean-Claude De Jaeger,[3] and Abdallah Ougazzaden[1,2,a)]

[1]*School of Electrical and Computer Engineering, Georgia Institute of Technology, Atlanta, Georgia 30324-0250, USA*
[2]*UMI 2958 Georgia Tech-CNRS, Georgia Tech Lorraine, 2-3 rue Marconi, 57070 Metz-Technopôle, France*
[3]*IEMN-CNRS 8520, PRES Université Lille Nord de France, Avenue Poincaré, Cité Scientifique, 59652 Villeneuve d'Ascq, France*
[4]*Laboratoire Matériaux Optiques, Photonique et Système, EA 4423, Université Paul Verlaine and Supélec, 2 rue E. Belin 57070 Metz, France*
[5]*Alcatel-Thales III-V Laboratory, 91461 Marcoussis, France*

(Received 27 March 2012; accepted 20 May 2012; published online 13 June 2012)

A GaN/ultrathin BGaN/GaN heterojunction is used in AlGaN/GaN high electron mobility transistors (HEMTs) to provide an electrostatic barrier to electrons and to improve the confinement of the 2-dimensional electron gas. BGaN back-barrier layers limit leakage in the GaN buffer thanks to two effects: a polarization-induced band discontinuity and a resistive barrier originating from excellent insulation properties of BGaN. Compared to conventional AlGaN/GaN HEMTs, structures grown with BGaN back-barrier showed a significant improvement of static performances, transport properties, and trapping effects involving a limited current collapse in dynamic regime. A DC maximum current increase of 58.7% was observed. © *2012 American Institute of Physics*. [http://dx.doi.org/10.1063/1.4729154]

Superior power and frequency handling capabilities of nitride high electron mobility transistors (HEMTs) make them an excellent technology for power-switching and millimeter-wave applications. In conventional AlGaN/GaN structures, bulk GaN comprises the buffer, but also serves as the electron carrier channel, which is located close to the interface. The intrinsic drawback of this design is that, even though electrons cannot spillover in the barrier, they do not encounter any potential barrier at the backside of the 2D electron gas (2DEG), resulting in buffer leakage. Additionally, the unintentional doping in GaN and the high threading dislocations rate favor the current leakage phenomenon[1] and limit the output power at high-frequency operation. Thus, to further enhance the mobility and lower the resistivity encountered by the 2DEG, one must improve confinement and the insulation of the buffer layer. This can be accomplished by compensation with dopants (Fe, C,…) (Refs. 2 and 3) or with the use of wide band gap materials such as AlN,[4] AlGaN, or double-heterojunctions (or DH-HEMTs).[5,6] However, these techniques necessitate extended thicknesses and are known to introduce deep-level defects in the buffer layer, resulting in current collapse at high voltage and high frequency.[7,8]

Alternatively, an InGaN ultrathin layer (1–3 nm) can be inserted in the GaN buffer as a back barrier to electrons to improve the confinement in the 2DEG.[9,10] In this case, to limit fast ramp-ups impeding structural quality,[11] a trade-off consists of increasing the InGaN barrier's growth temperature (~900 °C) (Ref. 12) and in lowering the GaN channel's (InGaN growth temperature is near 700–800 °C (Ref. 13) compared to 1000–1100 °C (Ref. 14) for GaN/AlGaN).

In this paper, we investigate the influence of BGaN back-barriers (BGaN BBs) in the buffer layer of conventional AlGaN/GaN HEMTs. It was shown that BGaN BB layers are highly resistive with only a few percent of boron (i.e., 0.65%–5%) (Ref. 15) and can potentially prevent carriers from leaking into the buffer. Moreover, optimal growth of BGaN materials by metal-organic chemical vapor deposition (MOCVD) is done at the same temperature than those used for AlGaN and GaN materials, ensuring higher structural and interfacial quality.

We performed simulations of band diagrams with a Schrödinger-Poisson solver[16] modified to accept BGaN materials. At less than 5% of boron content, few BGaN properties differ from those of pure binary GaN. Most significantly, the BGaN band gap exhibits a bowing and becomes smaller than that of GaN (as InGaN).[17] The conduction band and carrier concentration profiles obtained for a typical nitride HEMT structure including a BGaN BB of 5 nm with 1% of boron content are shown in Fig. 1 (physical constants used for calculation are found in Refs. 18 and 19). As the lattice parameter of BGaN tends to be smaller with boron incorporation compared to GaN, the density of created charges at the buffer/BB interface is negative unlike the case of InGaN barriers. Consequently, the conduction band is raised locally by about 0.11 eV, similarly to AlGaN barriers in DH-HEMTs, but this effect is not spread over the buffer as for InGaN.

In addition to this, resistivity of BGaN is significantly different from that of GaN as it increases drastically up to 10^5 Ω cm, with just a few percent of boron.[15] Thus, the thin layer of BGaN creates not only an electrostatic barrier, but also a resistive barrier to electrons between the channels enclosing the 2DEG and the GaN buffer below. The interplay of these two effects should ensure a better confinement of the sheet carrier concentration in the channel compared to conventional AlGaN/GaN HEMTs. Additional simulations showed a linear dependence of the electrostatic discontinuity's

a)Electronic address: abdallah.ougazzaden@georgiatech-metz.fr.

 © 2012 American Institute of Physics

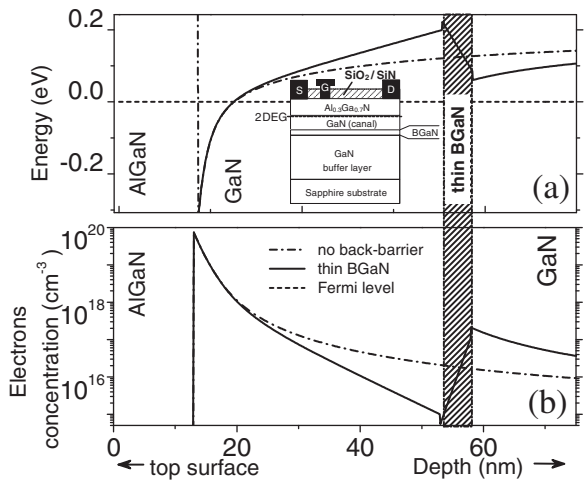

FIG. 1. Conduction band profile and carriers density for an AlGaN/GaN HEMT with and without a thin BGaN BB from the top surface to the buffer. The grey-colored area corresponds to the thin BGaN layer.

height with the BGaN BB thickness. Therefore, with a thinner barrier, the electrostatic effect becomes negligible and resistivity must predominate to account for the enhanced confinement, as later observed in our experiments.

Several AlGaN/GaN structures were grown with a BGaN BB.[20] We obtained high-quality material and negligible trap concentration for a thin BGaN BB with a 1 nm thickness, a boron content of 1%, and at a distance of 40 nm from the AlGaN/GaN interface.

First results of DC current-voltage characteristics between two electrodes deposited on the GaN buffer layer with and without a $B_{0.01}Ga_{0.99}N$ BB are shown in Fig. 2. We observe that the insertion of this ultrathin BGaN BB in the buffer layer reduces the leakage current of an order of magnitude for a large electric field range.

To further evaluate the influence of BGaN, we fabricated a set of epitaxial structures with and without a BGaN BB ultrathin layer. We employed commercial GaN templates composed of an AlN/GaN nucleation layer on sapphire substrate and a 3.5 μm undoped GaN buffer. For the first structure presented in this paper, the epitaxial growth started with a 400 nm GaN layer followed by a 1 nm $B_{0.01}Ga_{0.99}N$ BB, a 40 nm undoped GaN channel, and a 21 nm undoped $Al_{0.3}Ga_{0.7}N$ barrier layer (t_{AlGaN}). The second structure was grown as a reference with

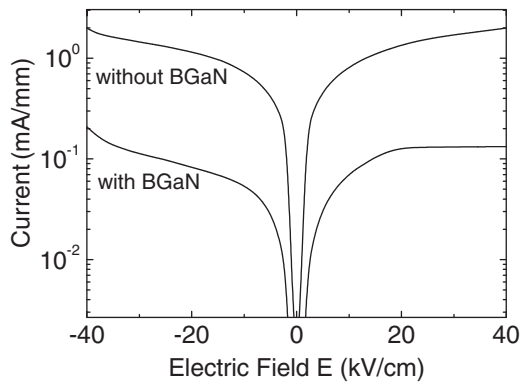

FIG. 2. Current-electric field characteristics between two electrodes performed on GaN buffer layer without and with BGaN BBs (GaN(40 nm)/$B_{0.01}Ga_{0.99}N$(1 nm)/GaN buffer layer).

the same epitaxy but with no BGaN BB. Surface roughness obtained by atomic force microscopy exhibited similar values for both structures suggesting no deterioration with the introduction of the BGaN layer.

For device fabrication, the source and drain were defined by e-beam lithography. The metallization used was based on evaporated Ti/Al/Mo/Au (12/200/40/100 nm) multilayer followed by a rapid thermal annealing at 900 °C for 30 s under nitrogen atmosphere. The device isolation is obtained by He^+ ions multiple implantations. The T-shaped gates were defined by e-beam lithography with a tri-layer resist stack, and the metallization used was based on evaporated Pt/Mo/Au (25/25/200 nm). Devices were passivated with a SiO_2/Si_3N_4 (100/50 nm) bi-layer dielectric deposited by plasma-enhanced chemical vapor deposition at 340 °C.[21]

Hall measurements performed on the HEMT structures without and with a BGaN BB exhibited sheet carrier densities of $7.5 \times 10^{12}\,cm^{-2}$ and $1.03 \times 10^{13}\,cm^{-2}$, electron mobilities of 906 $cm^2\,V^{-1}\,s^{-1}$ and 1230 $cm^2\,V^{-1}\,s^{-1}$, and a sheet square resistances of 851 Ω and 604 Ω at room temperature, respectively. These results clearly establish a notable improvement of the carrier confinement with the introduction of the BGaN BB. As the electrostatic barrier of 1 nm is relatively small, this improvement can be attributed to the resistivity of the BGaN BB, probably due to the decrease of the residual doping and the improvement of the material quality. This was confirmed by SIMS results obtained by Kim *et al.*[22] showing that the oxygen concentration in samples increases with the aluminum rate during the growth of AlGaN barrier layer, but drastically decreases when boron is incorporated.

For the HEMT including the BGaN BB, transmission line measurements showed a contact resistance of 0.56 Ω mm, a specific contact resistivity of $6.1 \times 10^{-6}\,\Omega\,cm^2$, and a sheet square resistance of 635 Ω at room temperature. A barrier height of 1.27 eV associated with an ideality factor of $\eta = 1.2$ was deduced from the forward characteristics of the Schottky contact. The reverse gate leakage was about 20 μA/mm at −10 V gate source bias. The breakdown voltage in transistor configuration was also greatly enhanced up to 190 V at pinch-off against 42 V for the device without BGaN BB for a gate-drain distance, $L_{GD} = 1\,\mu m$. Under three terminal voltage measurement, I_{DS} is improved by around two orders of magnitude at pinch-off from 4×10^{-3} A/mm to 7×10^{-5} A/mm. Regarding gate current, the gate leakage current drops of one order of magnitude (4×10^{-7} A/mm) with the BGaN BB at $V_{GS} = -6\,V$ and $V_{DS} = 10\,V$.

All DC and small signal measurements were carried out with a gate width of $2 \times 100\,\mu m$, a drain-gate spacing of 1 μm, a gate-source spacing of 0.5 μm, and a gate length (L_G) of 250 nm. The DC characteristics were measured with programmable alimentation multi-slots like HP4142 or Agilent 5270. DC measurement performed on the HEMT with BGaN exhibited a maximum drain current density of 642 mA/mm at $V_{GS} = 0\,V$ with an extrinsic transconductance (g_m) of about 137 mS/mm and a gate bias $V_{GS} = -3\,V$ for a drain bias $V_{DS} = 15\,V$. Small signal microwave measurements were also carried out on this transistor under probes. The calibration procedure was performed on wafer using a Through-Reflect-Match (TRM) method with a 40 GHz

Power Network Analyzer type E8363B. The S-parameters are measured in the 25 MHz to 40 GHz frequency range. The extrinsic current gain cut-off frequency f_t and maximum oscillation frequency f_{max} values are 30 GHz and 55 GHz, respectively, at $V_{DS} = 15$ V, $V_{GS} = -4$ V for a structure including a BGaN BB, but only 9.7 GHz and 36 GHz for the reference structure without BGaN.

Pulsed measurements were carried out for different quiescent bias points to study the trap response to an applied electrical field: ($V_{DS0} = 0$ V, $V_{GS0} = 0$ V) giving the reference characteristics, ($V_{DS0} = 0$ V, $V_{GS0} = -8$ V) showing the gate lag effect, and ($V_{DS0} = 15$ V, $V_{GS0} = -8$ V) showing the drain lag effect. The pulse duration was 400 ns with a duty cycle of 0.4%. Figure 3 shows an example of pulsed $I_{DS}(V_{GS},V_{DS})$ characteristics for two samples with and without a BGaN BB. In this case, the trapping phenomenon is reduced for the sample with BGaN BB, which exhibits excellent behavior at high frequency. At $V_{DS0} = 4$V, the current drop is 25.8% and 6.2% due to the gate and drain lag effects, respectively.

The extrinsic current gain cut-off frequency response can be defined by $f_t = v_{eff} \times (2\pi L_{G,eff})^{-1}$, where v_{eff} is the effective electron velocity and $L_{G,eff}$ is the effective gate length, with $L_{G,eff} = L_G + L_{GF}$, where L_{GF} is the fringing-field gate length. The electron velocities v_{e-eff} deduced from the extrinsic device measurement give 0.81×10^7 cm/s and 0.45×10^7 cm/s with and without a BGaN back-barrier, respectively. L_{GF} increases from 179 nm to 488 nm for structures with and without BGaN BBs. This result shows that the presence of the BGaN BB layer significantly reduces the surface density of states compared to the reference structure due to a drop of O_N acting as N doping. These values are determined without deembedding of the parasitic elements and must be compared with 1.24×10^7 cm/s from Jessen *et al.*,[23] which demonstrated sheet resistances between 25 kΩ and 304 MΩ for bulk BGaN material with 400 nm thickness. But, in this case, the growth was quasi-3D, which is incompatible with a transistor epitaxy. In our case, by including a 1 nm with 1% BGaN BB in the GaN buffer layer, the growth remains 2D and the sheet resistance increases from 25 kΩ up to 270 kΩ. These results show that BGaN BBs improve the electrons confinement in 2DEG and could reduce both the oxygen impurities in the heterostructure and the structural defects in the GaN channel. The difference between our results and those of Jessen *et al.*[23] is due to the strong short-channel effects and the material quality (indeed, the $f_t \times L_G$ product is 7.5 and the L_G/t_{AlGaN} aspect ratio is about 12). An electrostatic analysis demonstrates that electrons are pushed back behind the BGaN BB and cannot go through it because of its high resistivity. Consequently, charge concentration in the 2DEG is more confined in the quantum well and, therefore, the density and the mobility are greater.

In conclusion, we have presented designs for GaN based HEMTs with the introduction of BGaN back barrier layers. We found that the use of ultrathin BGaN BB with a thickness of 1 nm and a boron content of 1% drastically improves the electron confinement in standard AlGaN/GaN HEMTs and the resistivity of GaN buffer layer as well. These improvements significantly enhance the DC and RF performances of the transistors. Thus, a thick layer of BGaN, with 1%–5% boron content, creates an electrostatic and resistive barrier to electrons between the channels including the 2DEG and the GaN buffer below. This dual purpose of BGaN, being more suitable for MOCVD growth, shows that these innovative structures are very promising for high-power and high-frequency applications since an improved confinement of

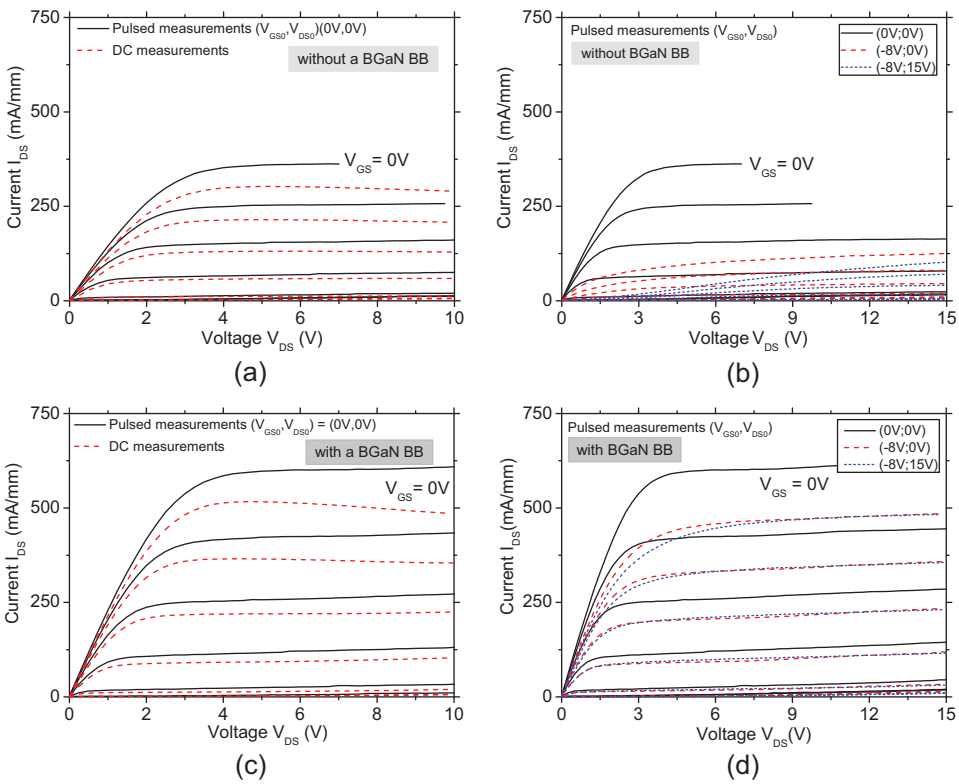

FIG. 3. $I_{DS}(V_{DS})$ measurement on DC and pulsed regimes on a device without [(a) and (c)] and with [(b) and (d)] an ultrathin BGaN BB. (a) and (b) DC measurement and pulsed with quiescent point at (V_{GS},V_{DS}): (0 V,0 V); (c) and (d) DC measurement and pulsed with quiescent point at (V_{GS},V_{DS}): (0 V,0 V), (−8 V,0 V), and (−8 V,15 V).

carriers can be obtained. As boron alloying in GaN layers significantly increases resistivity, BGaN can play a double-role as a back-barrier.

This work was supported by the National Research Agency (ANR) through the GABORE project (BLAN07-1-203576).

[1]C. Wetzel, T. Suski, J. W. Ager, E. R. Weber, E. E. Haller, S. Fischer, B. K. Meyer, R. J. Molnar, and P. Perlin, Phys. Rev. Lett. **78**, 3923 (1997).
[2]S. Heikman, S. Keller, S. P. DenBaars, and U. K. Mishra, Appl. Phys. Lett. **81**, 439 (2002).
[3]J. B. Webb, H. Tang, S. Rolfe, and J. A. Bardwell, Appl. Phys. Lett. **75**, 953 (1999).
[4]Z. Y. Fan, J. Li, M. L. Nakarmi, J. Y. Lin, and H. X. Jiang, Appl. Phys. Lett. **88**, 073513 (2006).
[5]C. Q. Chen, J. P. Zhang, V. Adivarahan, A. Koudymov, H. Fatima, G. Simin, J. Yang, and M. A. Khan, Appl. Phys. Lett. **82**, 4593 (2003).
[6]R. Chu, Y. Zhou, J. Liu, D. Wang, K. J. Chen, and K. M. Lau, IEEE Trans. Electron Devices **52**, 438 (2005).
[7]H. Yu, S. B. Lisesivdin, B. Bolukbas, O. Kelekci, M. K. Ozturk, S. Ozcelik, D. Caliskan, M. Ozturk, H. Cakmak, P. Demirel, and E. Ozbay, Phys. Status Solidi A **207**, 2593 (2010).
[8]A. P. Zhang, L. B. Rowland, E. B. Kaminsky, V. Tilak, J. C. Grande, J. Teetsov, A. Vertiatchikh, and L. F. Eastman, J. Electron. Mater. **32**, 388 (2003).
[9]J. Liu, Y. Zhou, J. Zhu, Y. Cai, K. M. Lau, and K. J. Chen, IEEE Trans. Electron Devices **54**, 2 (2007).
[10]T. Palacios, Y. Dora, A. Chakraborty, C. Sanabria, S. Keller, S. P. DenBaars, and U. K. Mishra, Phys. Status Solidi A **203**, 1493 (2006).
[11]Y. Wang, X. J. Pei, Z. G. Xing, L. W. Guo, H. Q. Jia, H. Chen, and J. M. Zhou, J. Appl. Phys. **101**, 033509 (2007).
[12]T. Palacios, A. Chakraborty, S. Heikman, S. Keller, S. P. DenBaars, and U. K. Mishra, IEEE Electron Devices Lett. **27**, 13 (2006).
[13]T. Matsuoka, N. Yoshimoto, T. Sasaki, and A. Katsui, J. Electron. Mater. **21**, 157 (1992).
[14]S. Nakamura, Jpn. J. Appl. Phys., Part I **30**, L1705 (1991).
[15]T. Baghdadli, S. Ould Saad Hamady, S. Gautier, T. Moudakir, B. Benyoucef, and A. Ougazzaden, Phys. Status Solidi C **6**, S1029 (2009).
[16]I.-H. Tan, G. L. Snider, L. D. Chang, and E. L. Hu, J. Appl. Phys. **68**, 4071 (1990).
[17]A. Ougazzaden, S. Gautier, T. Moudakir, Z. Djebbour, Z. Lochner, S. Choi, H. J. Kim, J. H. Ryou, R. D. Dupuis, and A. A. Sirenko, Appl. Phys. Lett. **93**, 083118 (2008).
[18]K. Shimada, T. Sota, and K. Suzuki, J. Appl. Phys. **84**, 4951 (1998).
[19]F. Bechstedt, U. Grossner, and J. Furthmuller, Phys. Rev. B **62**, 8003 (2000).
[20]A. Ougazzaden, S. Gautier, C. Sartel, N. Maloufi, J. Martin, and F. Jomard, J. Cryst. Growth **298**, 316 (2007).
[21]M. Mattalah, A. Soltani, J.-C. Gerbedoen, Az. Ahaitouf, N. Defrance, Y. Cordier, and J.-C. De Jaeger, Phys. Status Solidi C **9**, 1083–1087 (2012).
[22]H. Kim, F. J. Fälth, and T. G. Andersson, J. Electron. Mater. **30**, 1343 (2001).
[23]G. H. Jessen, R. C. Fitch, J. K. Gillespie, G. Via, A. Crespo, D. Langley, D. J. Denninghoff, M. Trejo, and E. R. Heller, IEEE Trans. Electron Devices **54**, 2589 (2007).